Study of the magnetic properties of nanoparticles interacting with surface acoustic waves

Author: Martí Checa Nualart[a)].
Advisors: Javier Tejada[a)] and Alberto Hernández[b)].
[a)]*Grup de Magnetisme, Departament de Física Fonamental, Facultat de Física, Universitat de Barcelona, Spain.*
[b)]*Paul-Drude-Institut für Festkörperelektronik, Berlin, Germany.*

In this work we design and build from zero, a device with the aim of studying the spin-phonon interaction in magnetic nanoparticles. New techniques to manipulate the magnetic moments of nanostructures are demanding to be studied. Surface acoustic waves (SAWs) are an excellent candidate as they offer a dynamic and tunable mechanism for the control of low energy excitations. The final goal of the project is to get closer towards acousto-magnetic devices as well as the better understanding of the fundamentals of the interaction. Both the design and building of the samples have been made by us at Paul-Drude-Institut für Festkörperelektronik in Berlin, with the idea of having an exhaustive control of all the parameters. Fe_2O_3 magnetic nanoparticles were embedded in a SiO_2 matrix, and deposited in a piezoelectric substrate ($LiNbO_3$) between two interdigital transducers (IDTs) that generate SAWs when they are connected to a source of microwaves. Magnetic measurements are taking place in a SQUID magnetometer at University of Barcelona, consisting in studying the magnetization dynamics when applying SAWs of different frequencies and powers to the sample. The effects of the temperature and the external applied field are also studied.

I. INTRODUCTION

Magnetic single domain nanoparticles (NPs), are becoming a hot topic in last years physics research due to both the wide range of applications where they are used (medical applications, sensors, electronic devices...), and the interest in low dimensional systems from a fundamental point of view. There is a strong demand of new techniques to manipulate their magnetic moments easily. For this aim, surface acoustic waves (SAWs) are a promising candidate, as they offer a dynamic and tunable mechanism for the control of low energy excitations.

The interaction of SAWs with magnetic materials like diluted magnetic semiconductors or ferromagnetic layers has been deeply studied in recent years[1-3]. The motivation of our work is the possible application in the technology world of the effects associated with this interaction.

SAWs are elastic deformations propagating along the surface of an elastic body, in our case the piezoelectric material $LiNbO_3$. Thus, they carry both an elastic wave and a voltage wave in the material. Since their amplitude decays rapidly into the bulk, the acoustic energy which is carried by the SAW is highly confined to a depth of around one wavelength below the surface. They have achieved a tremendous importance in the nanotechnology world due to their applicability in charge and spin transport in semiconductors[4].

Thus, we are interested in the study of the magnetic dynamics of NPs under acoustic fields at both low and room temperature. In the case of low temperatures, the possible occurrence of quantum phenomena deserves to be explored. For our project we will use Fe_2O_3 NPs slightly covered with an organic coating.

In this work, we design and build from zero the devices to perform this study and we characterize them from both a magnetic and an acoustic point of view. We also have started the study of the interaction between SAWs and magnetization. At the end of the work we show very preliminary results and we explain the next steps in this research line for further investigations.

The paper is organized as follows. In section II we give a qualitative idea of the theoretical framework of the project. The explanation of the experimental setup appears in section III. The samples preparation and characterization are explained in sections IV and V respectively, and the acousto-magnetic experiments appear in section VI. Finally the conclusions and further research are discussed in section VII and VIII.

II. THEORETICAL FRAMEWORK

Even though the work has an intrinsic experimental character, it is important to have a general idea of the fundamentals of the possible interaction of SAWs with NPs. The dynamics of the magnetic moment ($\mathbf{m}$) normalized to unit, in a NP are governed by the Landau-Lifshitz-Gilbert equation (LLGE),

$$\frac{\mathbf{dm}}{\mathbf{dt}} = -\boldsymbol{\gamma}[\mathbf{m} \times \mathbf{H_{eff}}] - \boldsymbol{\alpha\gamma}\big[\mathbf{m} \times [\mathbf{m} \times \mathbf{H_{eff}}]\big],$$

where $\boldsymbol{\gamma}$ is the gyromagnetic ratio, $\boldsymbol{\alpha}$ is the dimensionless damping coefficient, and $\mathbf{H_{eff}}$ is the effective magnetic field. The idea is that the SAW is able to interact with the NP by adding changes to the effective field ($\mathbf{H_{eff}}$) that the magnetic moment feels. This effective field is calculated from the magnetic energy landscape ($\mathbf{E_m}$) of the particle as

$$\mathbf{H_{eff}} = -\frac{\mathbf{1}}{\boldsymbol{V}}\frac{\boldsymbol{\partial}\mathbf{E_m}}{\boldsymbol{\partial}\mathbf{m}}.$$

Thus, changes in the energy landscape caused by the SAW would affect the magnetic behavior of the NP. These changes may be due to a variety of physical phenomena. On the one hand, the stress wave would be able to interact with the NP by means of magnetoelastic

[a)] marti7_@hotmail.com

coupling, where the strain tensor of our sample, together with the magneto-elastic coefficient of the NP would mark the intensity of the interaction. A mechanical rotation of the NP could be also induced by the SAW and this should be reflected in a reduction of the magnetic momentum in the laboratory frame.

On the other hand, the interaction of the voltage wave (generated in the piezoelectric) with the NP has two different possible contributions. First, the time-dependent electric field generated by the SAW will induce a magnetic field that could interact via Zeeman effect with the magnetic moment. Nevertheless, the low intensity of such magnetic fields allows us to neglect it. Second, the coupling of the magnetization with the electric field could be provided by the rotation of the anisotropy axis of the NP, which always follows the electric polarization vector **P** of the NP. The interaction of **P** with the electric field **E** induces an additional term to the effective magnetic field in LLGE, which can be treated like an AC magnetic field.[5]

Beyond all, the phonons of the SAW will increase the temperature of the sample, highly related to the magnetic dynamics of the system. Then, we will be introducing another source of interaction with the magnetic moments.

As we see, the possible changes observed in the magnetization dynamics could have very different origins. Thus, discerning which contribution is the responsible of such changes is a non-trivial work.

III. EXPERIMENTAL SETUP

A piezoelectric substrate ($LiNbO_3$, 128° Y-cut) is excited by applying a microwave signal to two interdigital transducers (IDTs) that generate SAWs of different powers and frequencies[6]. The transducer is formed by a series of fingers spaced out with a periodicity of λ, which determines the fundamental frequency (f_0 = 112 MHz) of the acoustic waves that the IDT can generate in the $LiNbO_3$. We use a Portable Network Analyzer (PNA) as a source of microwaves to be applied to the IDTs, and an rf-superconducting quantum interference device (SQUID) installed in a He cryostat for the study of the magnetization dynamics of the NPs.

When the microwave generator emits a multiple frequency of f_0, the IDT transforms the microwave signal in vibrations travelling along the piezoelectric crystal, and a SAW is generated. The NPs will be situated in the path of the SAW, embedded in a SiO_2 matrix. Similar experimental setups have been used to study the spin-phonon interaction in molecular magnets[7-8].

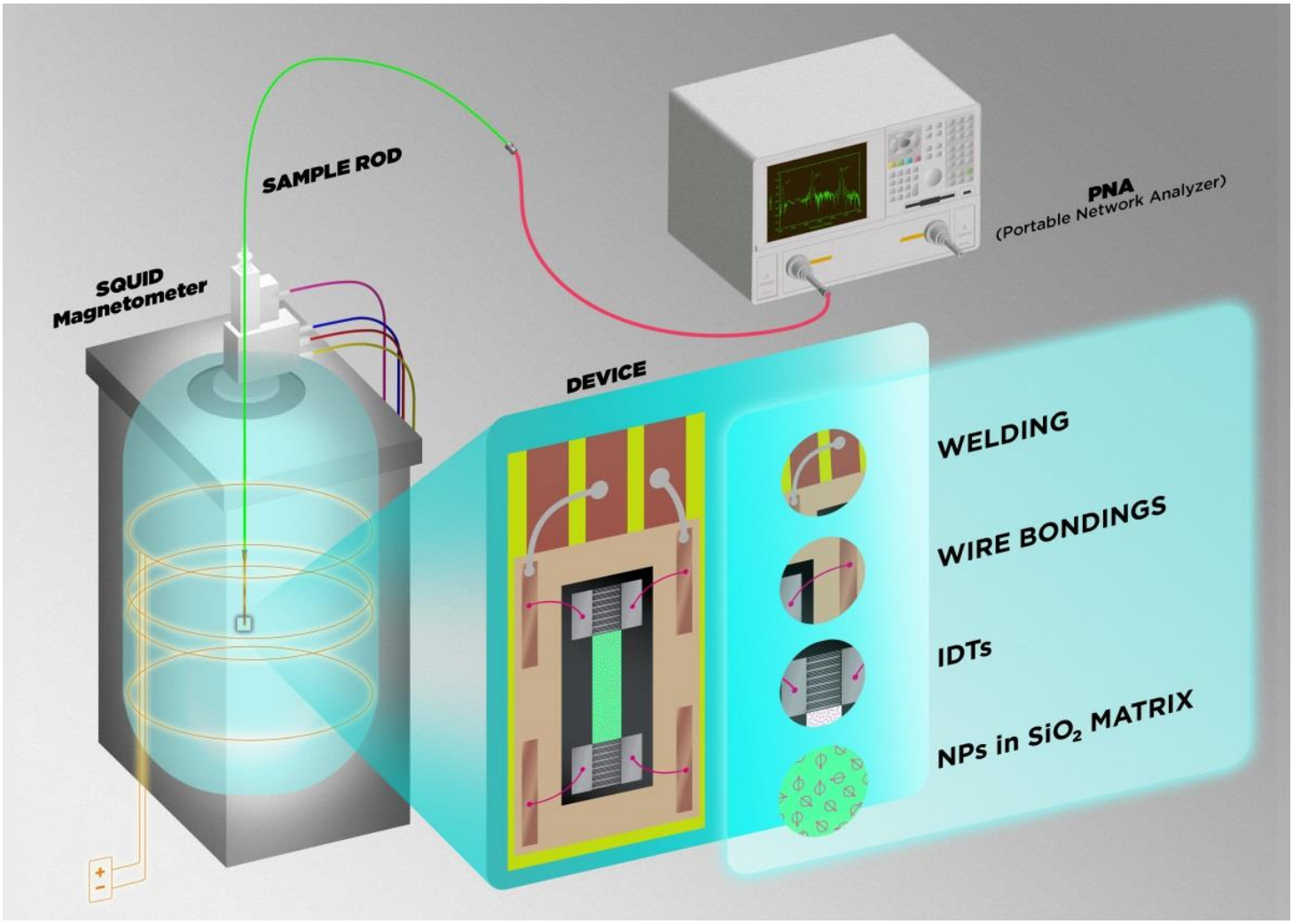

FIG. 1: Scheme of the experimental setup.

Therefore, we will study the evolution of the magnetization as a function of time (in a timescale ranging from microseconds to seconds) while we apply SAWs with different frequencies and powers.

Low and room temperature measurements will be performed in order to study the spin-phonon interaction in both the blocked and unblocked states of the NPs. The effect of an external applied field will also be studied.

A general scheme of the experimental setup is shown in FIG. 1.

IV. SAMPLE PREPARATION

In order to build the devices for our study, we needed to locate the single domain NPs along the SAWs propagation path in order to interact with the acoustic fields. The preparation of the samples was then divided in the three following steps: (A) fabrication of the IDTs on a piezoelectric substrate by means of lithography, (B) deposition of the NPs, and (C) cutting and bonding the structure to allow electronic access.

We performed all these steps ourselves, in the clean room of the Paul-Drude-Institut für Festkörperelektronik (Berlin).

IV.A IDTs lithography

There are several types of IDTs depending on the characteristics of the SAW that one wants to generate. The ones we built are called FEUDT (Floating Electrode Unidirectional Transducer), and are specially designed to obtain a unidirectional SAW in the piezoelectric (see structure in FIG. 2).

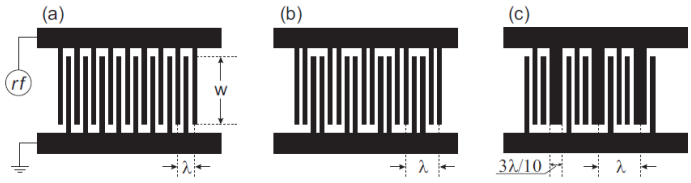

FIG. 2: Finger structure of the three most common types of IDTs. a) Single-finger (SF) IDT design. b) Double-finger (DF) IDT design. c) Floating electrode unidirectional IDT (FEUDT) design[6].

In FIG. 3 we show schematically the steps we followed to build them.

After cleaning the $LiNbO_3$ 128° Y-cut substrate in an oxygen plasma atmosphere, we dropped a few droplets of the photoresist (AR-N-7520/18) on it; we spun it at 4000 rpm and annealed it at 87°C, getting a thin layer of about 360 nm (panel A). Then, we had the sample ready for the lithographic mask alignment. Once the mask was aligned, we exposed the sample to UV light of 248 nm wavelength during 1.5 seconds (panel B). When the illumination was done, we baked the sample again at 87°C (panel C) and immersed it in the developer of the photoresist during 30 seconds (panel D). Distilled water was used to clean the developer off.

The three thin metal layers that form the IDTs were deposit on the sample by means of an evaporation process: 10 nm Ti, 40 nm Al, 10 nm Ti (panel E). Finally, we performed the resist lift off process by putting the sample in three different solutions: acetone (5 min), acetone (3 min), and isopropanol (3 min). The metal in the regions with resist was gone this way after the lift-off, leaving in the sample only the wanted metallic structure forming the IDTs (panel F).

The distance between two IDTs in a delay line (pair of IDTs located one in front of the other) is 2 mm. With respect to the longitude of the IDTs fingers, four different IDT sizes were built, with a length (w) of 424 µm, 212 µm, 106 µm and 53 µm, respectively.

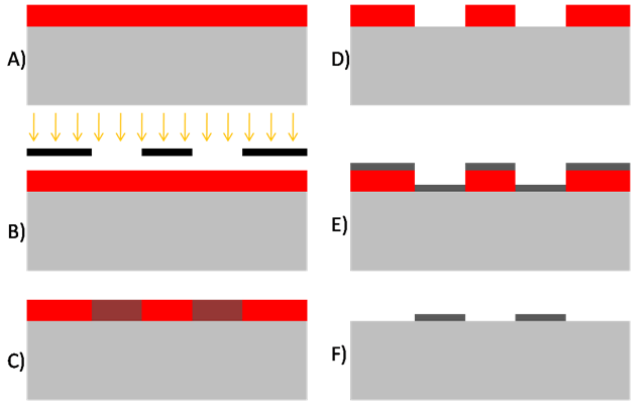

FIG. 3: IDTs lithography. A) Photoresist layer. B) Mask alignment and illumination. C) Post illumination baking. D) Developing process. E) Metal deposition. F) Lift-off.

In FIG. 4, one can see the aspect of a real sample (pictures were taken using an optical microscope). Each built wafer contains 5 delay lines.

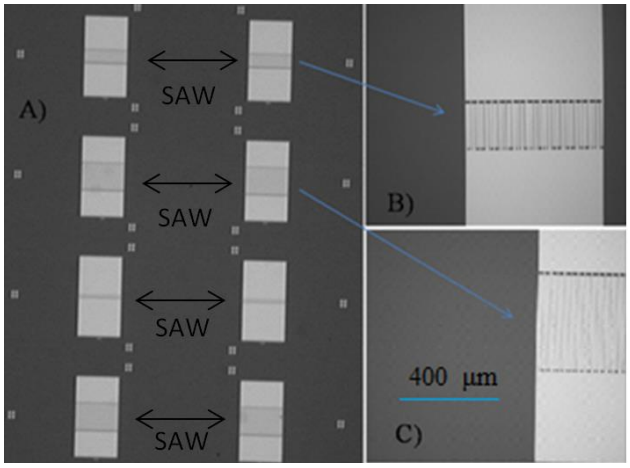

FIG. 4: Photo of the IDTs. A) Wafer with 4 delay lines. B) Zoomed in picture of the medium size IDTs. C) Zoomed in picture of the big size IDTs.

IV.B Nanoparticles deposition

The SAW generated in the piezoelectric is only travelling in the region between the IDTs and decays rapidly when we move away from it. So in order to avoid having contributions to the magnetic signal which are not going to be affected by the SAW, we have to design a procedure to locate the NPs only in the region where the SAW will be travelling.

Once the IDTs were built, we performed the NPs deposition. In FIG. 5 we schematically show the followed steps.

We covered the sample by spin coating at 4000 rpm with a 200 nm thin film of PMMA which is a non-photosensible resist, and baked it at 180°C. On top of this, we deposited a 1.5 μm thin film of a negative photoresist (also by means of spin coating at 3000 rpm) and annealed it at 87°C (panel A).

At this point, we opened a window in the path of the SAWs by illuminating the photoresist with a mask (panel B) and developing it (panel C). The PMMA window was opened by means of O_2 plasma etching using an ICP-RIE system at room temperature with an O_2 flow of 8 sccm (standard cm^3/min) during 2 minutes (panels D and E).

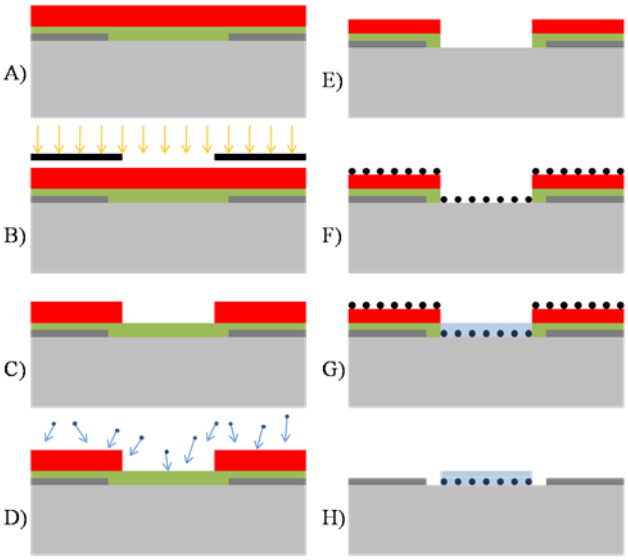

FIG. 5: Deposition method. Red color: Photoresist. Green color: PMMA. Light grey color: $LiNbO_3$. Dark grey color: IDTs. Light blue color: SiO_2. A) PMMA and photoresist layers. B) Mask alignment and illumination. C) Developing process. D) Plasma etching of the PMMA. E) Window opening. F) Nanoparticles deposition and spinning. G) Sputtering of SiO_2. H) Lift-off of the PMMA.

A solution containing the Fe_3O_4 nanoparticles was prepared, using n-hexane as a solvent in a concentration of 50 mg/mL. Therefore, the deposition was performed by dropping some droplets of the solution in the sample, using a micropipette and spinning it at 3000 rpm to try to avoid the agglomeration of NPs to obtain the maximum possible homogeneity (panel F).

Then, a 100 nm thin film of SiO_2 was sputtered in the region between the transducers using a shadow mask (in order to only sputter the desired region) fixing the NPs to the surface and embedding them in an amorphous solid matrix (panel G).

Finally the lift-off process using acetone was done, leaving in our device just the NPs embedded in the SiO_2 matrix, located in the region between the IDTs, where the SAW was going to travel (panel H).

In FIG. 6 you can see some real pictures of the process taken using an optical microscope.

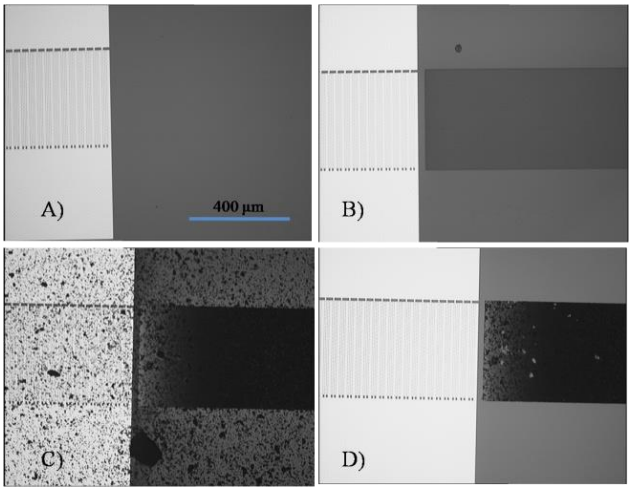

FIG. 6: A) IDTs with the PMMA and photoresist layers. B) Window opened. C) Nanoparticles deposition, spinning and SiO_2 sputtering. D) Final aspect after lift-off process.

Samples containing different NP concentrations where constructed by dropping different amounts of droplets of the magnetic solution during the process. The NPs deposition in our device was one of the most difficult processes during the work, because depending on the size and coatings of the NPs, they are not easily solved in the usually organic solvents (that is why we had to use n-hexane), and they tend to form micrometric clusters that cause the agglomeration of the magnetic material.

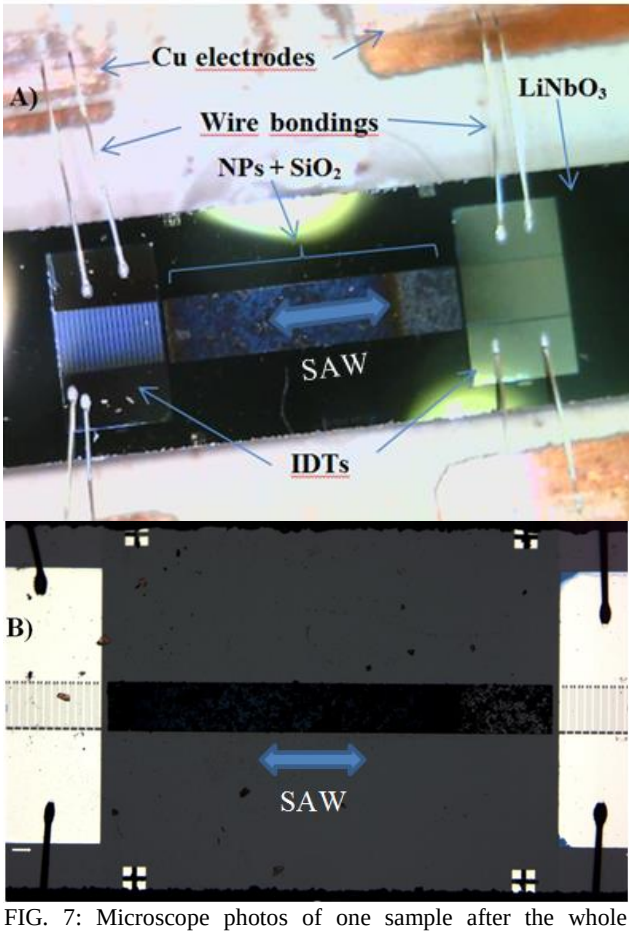

FIG. 7: Microscope photos of one sample after the whole process. A) Color photo. B) Black and white photo.

IV.C Cutting and bonding process

As the magnetic measurements would take place in a SQUID magnetometer, the size of the sample was strongly limited, so we had to cut our sample in single delay lines. To do so, we used either a hydraulic cutting machine or a diamond wire due to the high hardness of $LiNbO_3$. Using a wire bonding machine, we attached the transducers to a bigger metallic (Cu) electrode to be able to connect it to the ports of the PNA without breaking the sample. The wire bonds were made of Aluminum. The final aspect of the samples is shown in FIG. 7.

V. SAMPLE CHARACTERIZATION

Here, we present both acoustic and magnetic characterizations of the devices we built before starting the magneto-acoustic experiments.

V.A Acoustic characterization

We had to check whether the acoustic signal of the IDTs had changed after the whole procedure (see FIG. 8). To do so, we connected the two IDTs of one of our samples to the two ports of the PNA, and we sent a microwave signal while we measured the different modes (S11 or S12) of the PNA.

On the one hand, in the reflection mode (S11), we measure in logarithmic scale the ratio between the power applied to the IDT and the power reflected by the IDT. Thus, a downward peak in the spectra indicates that a part of the energy sent to the IDT is not being returned and is being used to generate a SAW. The different peaks correspond to the different harmonics of the fundamental frequency (f_0 = 112 MHz) of the IDT.

On the other hand, in the transmission mode (S12), we measure (also in logarithmic scale) the ratio between the power sent to one of the IDTs in a delay line and the power received in the opposite IDT. Thus, an upward peak in the spectra reveals that part of the energy sent to one of the IDTs is reaching the other IDT (through a SAW).

We observed that while the S11 was pretty much the same before and after the procedure, the S12 had some significant changes. The fact that the reflection signal was quite similar is telling us that the IDTs are not being damaged by the process and they are generating the SAWs properly.

However, with respect to the transmission signal, we observed that after the NPs deposition, the 3rd harmonic peak was not found, and the signal of the 1st and 2nd ones was weaker. These facts can have different origins. First, the randomly distributed NPs are somehow causing a scattering of the SAW that is making the transmission signal weaker. This scattering is stronger as the wavelength of the SAW decreases; this is why we do not see transmission for harmonics above the second one. Second, we also have to take into account the absorption of the acoustic energy that is causing changes in the magnetic behavior, making the transmission signal go down. Finally, the change in the acoustic properties between the substrate and the NPs + SiO_2 layer provokes damping of the SAW too.

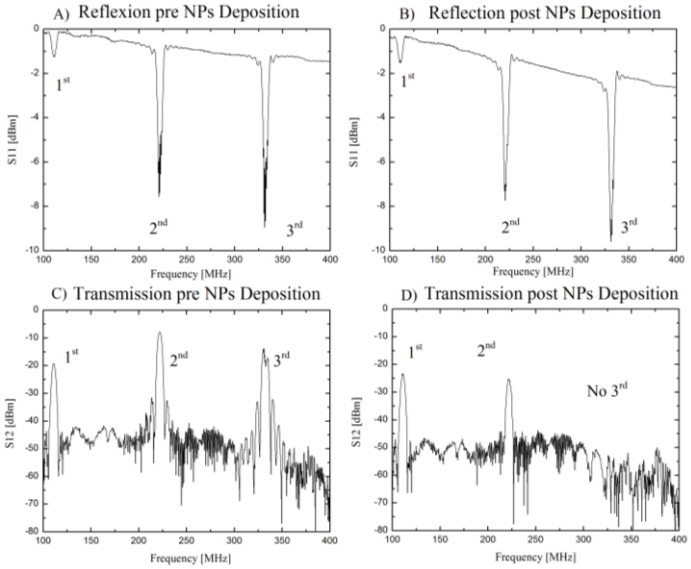

FIG. 8: IDTs response after and before the NPs deposition procedure. A) Reflection signal (S11) before the treatment. B) Reflection signal (S11) after the treatment. C) Transmission signal (S12) before the treatment. D) Transmission signal (S12) after the treatment.

V.B Magnetic characterization

We also characterized from a magnetic point of view the device we had built, before starting the acousto-magnetic experiments. The main defect that our samples have is that due to their thin film characteristics, and their small size, the magnetic signal coming from the deposited magnetic NPs is significantly low. Even though, using a SQUID magnetometer, one can measure the hysteresis loop of the sample at low and room temperature as well as the Zero-field-cooled-Field-cooled (ZFC-FC) curves (see FIG. 9).

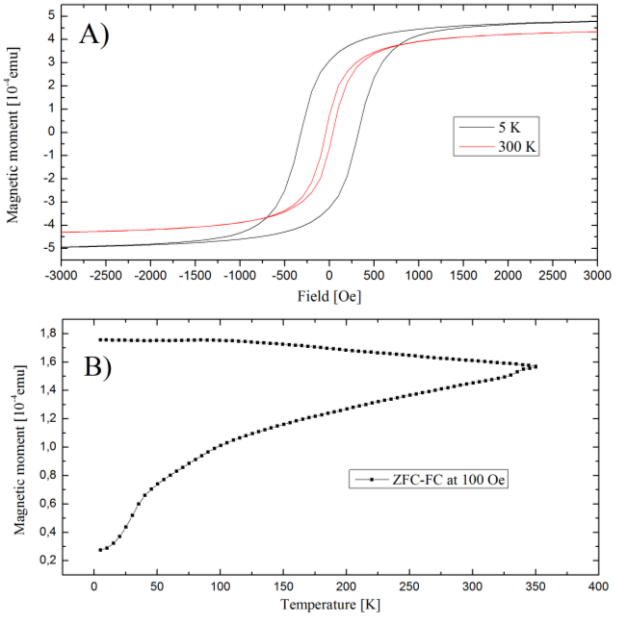

FIG. 9: Magnetic characterization. A) Hysteresis loops at low and room temperature. B) ZFC-FC curves at 100 Oe applied field.

We obtained the typical hysteresis loop of magnetic NPs; in this case they have a saturation field around 1500 Oe. The ZFC-FC measurement tells us that the blocking temperature of the NPs is around room temperature. Then, due to the relationship between the blocking temperature (T_B) and the volume (V) of the NP ($T_B = \frac{kV}{K_B \eta}$), where k is the magnetic anisotropy, and η is a parameter related to the measurement, one can obtain the size distribution function of the NPs. We obtained a typical radio around the tens of nm.

The attenuation in the acoustic transmission signal is directly related to the amount of magnetic material that we deposit in the piezoelectric. The samples with more magnetic material (having stronger magnetic signal) have a lower acoustic transmission signal. On the contrary, the samples with less magnetic material (lower magnetic signal) have a stronger acoustic transmission signal.

Thus, there is always a competition between both signals: if we try to increase the magnetic signal by depositing more NPs, we lose acoustic signal, and if we try to increase the acoustic signal by depositing less NPs, we lose magnetic signal.

VI. ACOUSTO-MAGNETIC MEASUREMENTS

A SQUID magnetometer as the one in the scheme of FIG. 1 is basically composed of three electric coils connected to a Josephson junction that acts as an extremely precise voltmeter to detect changes in the magnetic flux going across the coils.

The general setup to perform the acousto-magnetic experiments has been already explained in section III. The sample was placed at the end of the sample rod of the SQUID and the Cu contacts of our devices were properly welded to the coaxial cable descending by the rod, using a 60% tin, 40 % lead alloy.

Once the sample was inside the SQUID, one had to center it in order to get the maximum signal coming from the Josephson junction, which means moving the sample through the coils until it is located in the center of the middle coil. Due to the small magnetic signal of our samples, the centering step is quite difficult to perform. Unwanted paramagnetic or diamagnetic signals coming from the sample holder, the piezoelectric substrate, the wire bondings, the welding, the SQUID rod…, may be of the order of magnitude of the signal coming from the NPs, making the process more difficult.

The procedure to center was to apply a strong magnetic field until the NPs were saturated, and then remove it leaving the sample in its remnant state. What we expect with this is that the entire paramagnetic and diamagnetic spurious signals would go to zero, and only the signal coming from ferromagnetic materials (like our NPs) would contribute to the signal.

Then, we connected the coaxial cable of the SQUID rod (which is connected to the IDTs in the sample) to an ESG-D Series Signal Generator which sends microwave pulses of selectable frequency, power and duration. By choosing a frequency multiple of $f_0 = 112$ MHz, when the IDT receives the microwave pulse, it will generate a SAW in our device. At the same time, we also plugged the voltage signal of the magnetometer and the output signal of the Signal Generator to an oscilloscope, being able to watch both signals (the pulses and the magnetic changes) together.

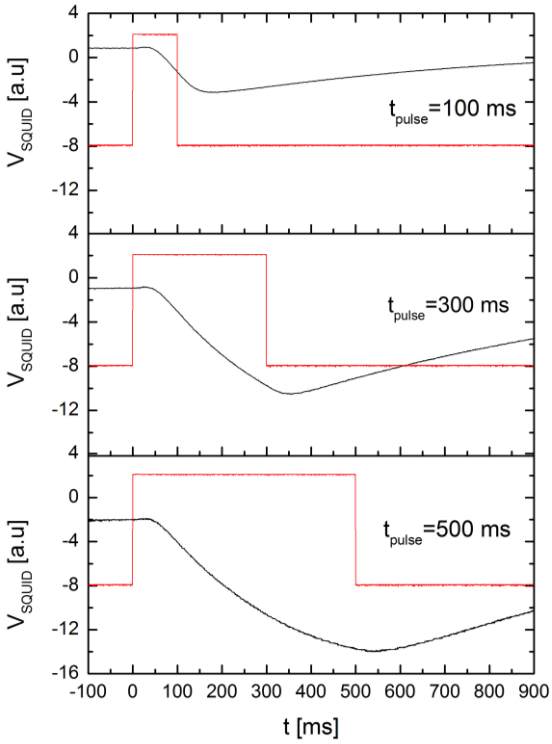

FIG. 10: In black, the SQUID voltage signal when we apply microwave pulses of 16 dBm with different widths at an applied field of 500 Oe and at a temperature of 5 K. In red, the microwave pulses sent to the device.

At this point, we look for changes in the signal of the SQUID, when the SAW pulses are applied under different values of rf frequency, rf power[9], pulse duration, magnetic field and temperature.

To the date, we have not found general conclusions of our study. Nevertheless, very preliminary results have been obtained. We find that under certain conditions, when a microwave pulse of one of the multiple frequencies of f_0 is sent to the IDT, a decrease in the voltage signal of the SQUID appears, indicating a change in the magnetization of the sample.

In FIGS. 10 and 11, we show this behavior as a function of the duration of the pulse and the power that we send, respectively. The measurements were performed at 5 K and at an applied field of 500 Oe. In both cases there is a clear relationship between the pulse sent and the decrease in the SQUID voltage signal, so the magnetization of the system. To perform these studies we chose the second harmonic of the IDT ($f = 2f_0 = 224$ MHz).

In FIG.10 we plot in black the SQUID voltage signal, and in red the microwave pulses sent to the sample. We can see that the magnetic changes increase with the duration of the pulse. We also observe that the SQUID response has always a delay of 30 - 40 ms with respect to the applied pulse.

In FIG.11 we plot in colors the SQUID voltage signal, and in black the microwave pulses sent to the sample. We observe that the magnetic changes increase with the power of the pulse. We also see the delay time already observed in FIG. 10.

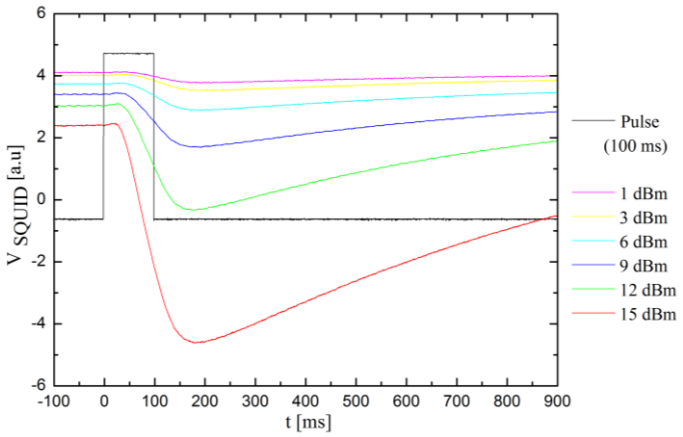

FIG. 11: In colors, the SQUID voltage signal when we apply a microwave pulse of different powers at an applied field of 500 Oe and at a temperature of 5 K. In black, the microwave pulse sent to the device.

The same study was performed as a function of the frequency of the microwave (see FIG. 12), finding only this decrease in the output voltage signal when the frequency is a multiple of f_0, that is when the IDT is generating a SAW. Thus, we think it is clear that the changes we see are being generated by the SAW.

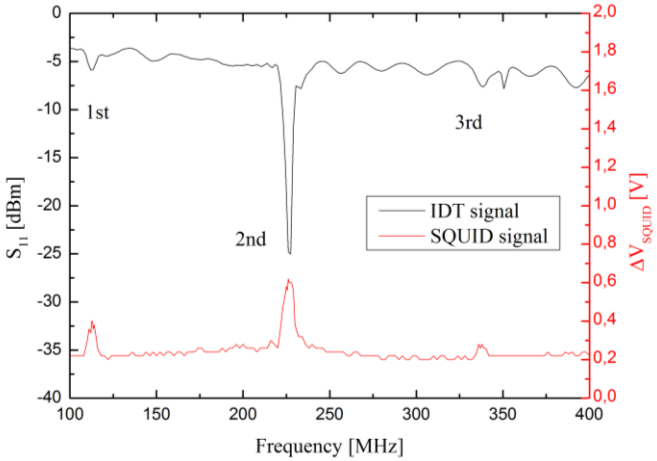

FIG. 12: In red, the decrease in the SQUID voltage signal when we apply a microwave pulse of 15 dBm and 50 ms width, as a function of the frequency at 10 K. In black, the S_{11} signal of the IDT as a function of the frequency.

The most important issue here is to discover if the SQUID signal that we get is coming from the NPs or if it is some spurious magnetic signal coming from another part of the experimental setup.

There are two facts that are preventing us to read these results from a more conclusive point of view. The first issue is that this behavior is only seen at low temperature and disappears above 15 K, suggesting there could be some material in the setup transiting to a superconductor state (it could be the tin and lead alloy used for welding) and giving a strong magnetic signal.

Besides, the other unexpected fact is found when we perform the study as a function of the magnetic field applied. We find that the decrease in the magnetic signal does not saturate when we increase the magnetic field, but increases steadily. If we go to high fields (2 - 5 T), the behavior is still found even more markedly, reaching changes in the voltage SQUID that are even bigger than the signal of the hole sample at its saturation point.

These two facts are what make us wonder the most whether the signal that we receive comes from our NPs or elsewhere in the experiment. It is possible that the SAW generated is heating up the sample and its nearby region, then the change in the temperature it is seen in the SQUID voltage as a change in the magnetization of a heated magnetic material.

This hypothesis would agree with the delay between the acoustic and magnetic signal. This delay could be the time it takes the energy to dissipate as heat and to arrive to the place where the magnetic material is. Candidates for giving this magnetic signal are the NPs, the tin and lead alloy used for welding, the piezoelectric substrate, the plastic support used as a sample holder, among others.

It is also possible that the magnetic response that we see is coming from more than one of those candidates, and the unexpected behaviors commented previously are a sum of all the magnetic contributions that we have. We are working to find out where this signal comes from, and also trying to build new samples with a stronger magnetic signal to finish with this ambiguity.

VII. CONCLUSIONS

The main conclusions that we get from this master thesis are the following:

i) Starting from zero, we have designed an interesting and useful device for the study of the interaction between surface acoustic waves and nanoparticles, by developing a process to deposit the magnetic material between 2 interdigital transducers in an acoustic delay line.

ii) We have proved that the nanoparticle deposition affects the acoustic transmission signal in our device.

iii) There is a magnetization variation at low temperatures when the SAWs are active. The origin of this variation is still unclear. New samples with stronger magnetic signal are needed to finish with this ambiguity, and also other techniques to study the magnetization dynamics could be interesting.

iv) The learning of the methodology to work in a cleanroom as well as the operation of a SQUID magnetometer and a Portable Network Analyzer has been achieved.

VIII. FURTHER RESEARCH

As it has been said, we should finish with the ambiguity of the results of the acousto-magnetic

experiments in the SQUID magnetometer and new samples with stronger magnetic signal are needed for this.

Thus, we are working in a new sample preparation method, with two different goals. First, to deposit the NPs on the piezoelectric without embedding them in the SiO_2 matrix, in order to see if the matrix is somehow affecting the spin-phonon interaction. Second, to deposit the NPs geometrically arranged in order to have all their anisotropy axes pointing in the same direction, having at the same time a stronger magnetic signal and avoiding NPs agglomeration.

On the other hand, in order to optimize the study of such phenomena, novel techniques such as X-ray magnetic circular dichroism (XMCD) are a very interesting candidate to study nanomagnetic interactions like the ones presented in this work. XMCD allows not only to study the magnetic behavior of small systems such as one single NP, due to its high magnetic sensitivity and spatial resolution, but also to study their dynamics at very small timescales (around the nano or even pico seconds), taking advantage of the extremely bright, coherent and short light pulses coming out of a synchrotron X-ray source. XCMD as a local technique would also allow us to finish with the ambiguity of not knowing where our signal comes from.

Acknowledgments

I would like to express my special thanks of gratitude to my advisors Dr. Javier Tejada and Dr. Alberto Hernández-Mínguez who gave me the golden opportunity to start working in this promising project, as well as the whole Group of Magnetism of the UB for helping me always in anything I need. I am also thankful to the group of Dr. Paulo Santos in PDI for making my stay in Berlin very pleasurable from both the scientific and personal point of view, and to Mr. Felipe Franco for helping me with the illustration of the experimental setup.

I would also like to thank my partner, family and friends who have always helped me a lot in finishing this final master project within the limited time.

[1] S.Davis, et al. "Magnetization dynamics triggered by surface acoustic waves". Applied Physiscs Letters **97**, 232507 (2010).

[2] L.Dreher, et al. "Surface Acoustic Wave-Driven Ferromagnetic Resonance in Nickel Thin Films: Theory and Experiment". Physical Review B **86**, 134415 (2012).

[3] Y.Yahagi, et al. "Controlling nanomagnet magnetization dynamics via magnetoelastic coupling". Physical Review B **90**, 140405(R) (2014).

[4] S. Büyükköse, et al. "High-frequency acoustic charge transport in GaAs nanowires". Nanotechnology **25**, 135204 (2014).

[5] Eugene M. Chudnovsky, et al. "Electromechanical magnetization switching". Journal of Applied Physics **117**, 103910 (2015).

[6] S. Büyükköse, doctoral thesis, "Nanoimprinted High-frequency surface acoustic waves devices" (2014).

[7] A. Hernández-Mínguez, et al. "Quantum Magnetic Deflagration in Mn12 Acetate". Phys. Rev. Lett. 95, 217205 (2005).

[8] J.M.Hernandez, et al. "Acoustomagnetic pulse experiments in LiNbO3 /Mn12 hybrids". Applied Physics Letters **88**, 012503 (2006).

[9] The use of dBm units is just a common way to express power in microwave measurements as $P(dBm)=10\log_{10}[P(mW)/1\ mW]$.